Supplement of Hydrol. Earth Syst. Sci., 23, 1409–1429, 2019
https://doi.org/10.5194/hess-23-1409-2019-supplement

Hydrology and Earth System Sciences
Open Access

Supplement of

Attributing the 2017 Bangladesh floods from meteorological and hydrological perspectives

Sjoukje Philip et al.

Correspondence to: Sjoukje Philip (sjoukje.knmi@gmail.com) and Geert Jan van Oldenborgh (oldenbor@knmi.nl)

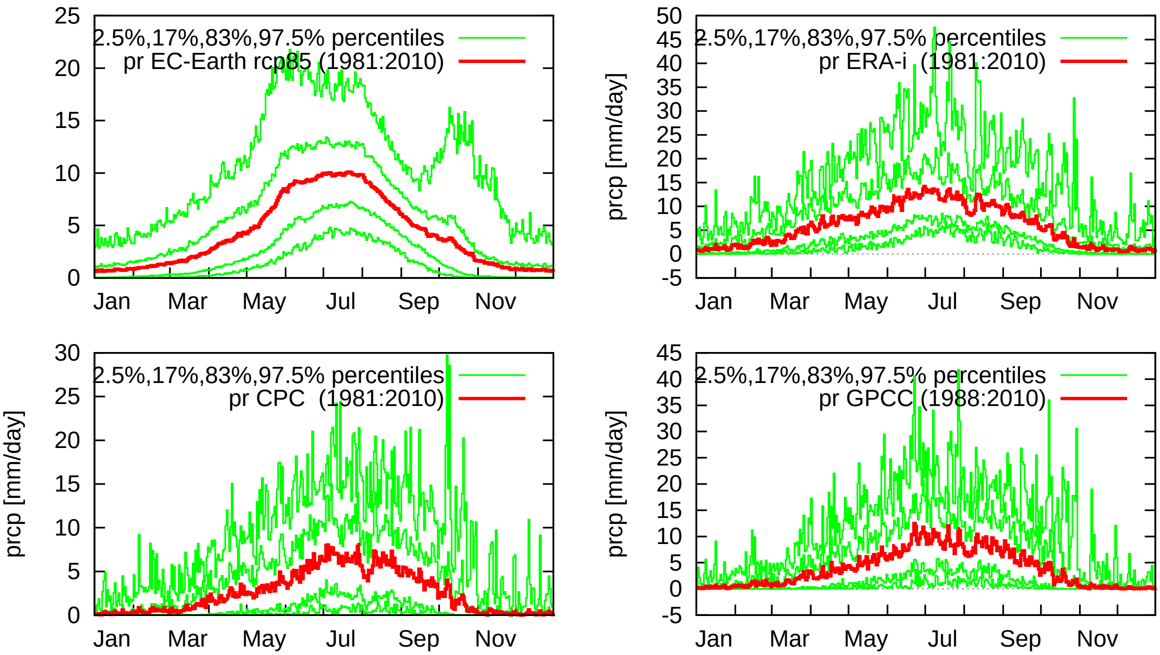

Figure S1. Seasonal cycle of EC-Earth (top left) and observational precipitation datasets wrt 1981-2010 (1988-2010 for GPCC). The red line shows the mean value, green lines show the 2.5, 17, 83 and 97.5 percentiles.

1 EC-Earth

We performed analyses with ensemble experiments from the coupled atmosphere-ocean general circulation model EC-Earth 2.3 (Hazeleger et al., 2012). The resolution of the model is T159, which is about 125 km.

We use three different EC-Earth-2.3 experiments. The first is a transient model experiment, consisting of 16 ensemble members covering 1861–2100 (here we use up to 2017), which are based on the historical CMIP5 protocol until 2005 and the RCP8.5 scenario (Taylor et al., 2012) from 2006 onwards. To compare these runs with observations, we use model years in which the difference in smoothed observed global mean surface temperature (GMST) between 2017 and a year in the past (1984, 1979, and 1900) agrees with the difference in ensemble averaged model-GMST between 2017 and that year in the past. These are the model years 1985 and 1979 (corresponding to 1984 and 1979 in observations) and 1934 (corresponding to 1900 in observations).

The other two EC-Earth-2.3 experiments are time slice experiments, based on the above 16-member transient model experiment. Two experimental periods are selected in which the model-GMST is as observed in 2011-2015 ('present-day' experiment, model years 2035-2039) and as pre-industrial (1851-1899) + 2 °C warming ('2°C-warming' experiment, model years 2062-2066). For each time slice, 25 members are generated from each of the 16 transient ensemble members and these are integrated for 5 years, resulting in $16 \times 25 \times 5 = 2000$ years of data for each time slice. The difference in model-GMST between the two time slice experiments is such that it is the same as the difference between the observed present-day GMST and a 2 °C warmer world.

Fig. S1 shows the seasonal cycle of daily rainfall for both observations (CPC, ERA-int and GPCC) and the EC-Earth model. It shows that in the model, as expected, most precipitation falls in the months JJA, with a peak in July, like in observations, though the increase in precipitation is slightly steeper in June than it is in observations. The average amount of rainfall in these months is comparable to the observational datasets, with a maximum of around 10 mm/day. It is worth noting that CPC tends to underestimate the precipitation at higher elevations due to a lack of available station data.

Table 1. Experiments with the weather@home ensemble, including ensemble size and short description.

Category	Experiment	Ensemble size	Description
Climatology	Historical	5222	1986-2015 SSTs and sea ice as observed, other forcings from CMIP5 historical+RCP4.5
	Natural	6659	1986-2015, SSTs reconstructed for pre-industrial, all other forcings pre-industrial
	GHG-only	4931	1986-2015, SSTs reconstructed for GHG emissions only, CMIP5 historical+RCP4.5 GHG emissions, all other forcings preindustrial
2017-Specific	Actual 2017	2996	2017 SSTs and sea ice as observed, other forcings as RCP4.5
	Natural 2017	6126	2017, SSTs reconstructed for pre-industrial, all other forcing pre-industrial
	GHG-only 2017	5386	2017, SSTs reconstructed for GHG emissions only, RCP4.5 GHG emissions, all other forcings preindustrial
Future	Current	2781	2004-2016, SSTs and sea ice as observed, all other forcings from CMIP5 RCP4.5 as per HAPPI experiment design
	1.5 Degree	1848	Representative decade with 1.5° C of additional warming as per HAPPI experiment design
	2.0 Degree	1892	Representative decade with 2° C of additional warming as per HAPPI experiment design

2 weather@home

Large ensembles of climate model simulations are created using the distributed computing weather@home modelling framework (Guillod et al., 2017; Massey et al., 2014). The weather@home setup consists of the Met Office Hadley Centre Atmosphere-only model, HadAM3P running globally at a resolution of $1.25° \times 1.875°$ to drive the Met Office Hadley Centre Regional Model, HadRM3P running at a resolution of 50 km over South Asia. The model is driven with prescribed sea surface temperatures (SSTs) and sea ice (SIC). Table 1 describes the experiments used in this study, which are grouped into three sets - (i) ensembles for the historical period 1986-2015, (ii) ensembles for 2017, (iii) ensembles for assessing possible changes in the future.

The first set of climatology experiments captures the years 1986-2015. To derive the value of the observed threshold within the weather@home model a climatology (with each year run independently) from 1986-2015 is run using observed OSTIA SSTs and SIC (Donlon et al., 2012) and CMIP5 historical+RCP4.5 estimates of other forcings (hereafter, Historical). A second climatology representing pre-industrial conditions is run from 1986-2015 using observed OSTIA SSTs and SIC naturalised as above with CMIP5 estimates and pre-industrial CMIP5 forcing conditions (hereafter, Natural). The Natural ensemble is constructed following Schaller et al. (2016), where the anthropogenic signal in the SST is derived from the difference between historical and historicalNat CMIP5 simulations from 13 different models and removed from the observed SSTs. A third ensemble (hereafter, GHG-only) is also included for the years 1986-2015, where GHG emissions follow the same protocol as for the Historical ensemble, but all other forcing components are kept at pre-industrial levels as for the Natural ensemble. As with the Natural component, the signature of GHG emissions in the SST is removed by comparing the relevant CMIP5 simulations to obtain a set of plausible SST patterns. The SSTs are specifically reconstructed to respond to changes in GHG emissions only, without the influence of the historical changes in other anthropogenic forcings.

The second category of 2017-specific experiments simulate the year 2017 for three different ensembles. One ensemble simulates the world as observed for 2017 (hereafter Actual 2017) taking observed OSTIA SST and SIC to drive the model and with sulphate emissions, well-mixed greenhouse gas, solar variability and volcanic emissions taken from CMIP5 values. A counterfactual ensemble (hereafter Natural 2017) is run for 2017 and uses pre-industrial forcing estimates as Natural above. A third ensemble for GHG only in 2017 also generated as above (hereafter GHG-only 2017). The difference between the GHG-only 2017 simulations and the Actual 2017 experiments is the inclusion of the anthropogenic sulphate emissions, so by comparing the two simulations it is possible to derive an estimate of the anthropogenic aerosol influence. We have successfully tested the assumption of linearly additive forcing responses using a small subset of CMIP5 Aerosol only experiments.

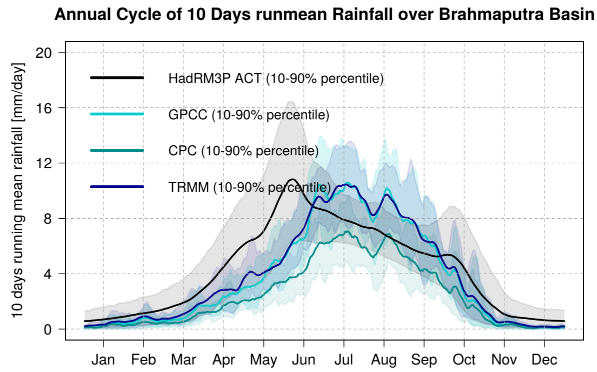

Figure S2. Annual cycle of 10-day running mean rainfall in the Brahmaputra region for weather@home output and CPC, CPCC and TRMM datasets.

A third category of future experiments are performed with weather@home 'South Asia' following the HAPPI experimental design (Mitchell et al., 2017) where a decade of simulations are performed representing a world as currently observed (hereafter Current), and with global mean surface temperature increase limited to 1.5° C and 2° C above pre-industrial levels (hereafter 1.5 Degree and 2 Degree respectively). Although the simulation period is only 10 years (adding future SST pattern onto OSTIA SSTs for 2006-2015), the HAPPI model setup is comparable with the climatological and 2017 experiments.

The annual cycle of 10-day running mean precipitation in the Brahmaputra basin from weather@home Historical simulations is compared to CPC, GPCC and TRMM observational records in figure S2. Note TRMM is also included for reference but since data is not available post 2015 it is excluded from the rest of the analysis. Within the monsoon season the mean magnitude of precipitation within weather@home shows reasonable agreement with observational estimates, although the variability of precipitation in this period is too small. In the pre-monsoon season weather@home precipitation is too high and therefore the monsoon onset appears to occur too early within the model. Comparing the spatial agreement of JJAS mean precipitation (not shown) shows that, although model output is noisier, the magnitude and pattern of weather@home output agrees well with GPCC and CPC observations.

3 PCR-GLOBWB

In this study we used the global hydrological model PCR-GLOBWB 2 (Sutanudjaja et al., 2017). This model was selected because of its ability to simulate the hydrological cycle, including reservoir operations and human water interactions at continental and global scales. The model simulates the global water balance at daily temporal resolution and at either 10 km or 50 km spatial resolution. It resolves the water balance at the surface, by using precipitation, temperature and potential evaporation inputs from meteorological observations or climate models.

PCR-GLOBWB calculates the vertical flow between soil layers and from the unsaturated to the saturated zone. It uses observed vegetation properties and land use dynamics to solve the water balance at the global scale for every 10× x 10 km grid cell. The runoff from each location, flows along a topography driven drainage network to the outlet of the river basins. Over 6000 reservoirs and lakes are included in the drainage network to provide accurate simulations of river discharge in human modified river systems. Human water abstractions for irrigation, livestock, household and industry are included in the model.

We used PCR-GLOBWB to conduct several river discharge simulations as explained hereafter. Firstly we checked the performance of the model by comparing the output to observations of (i) the 2017 event, (ii) other historical flooding events and (iii) river discharge over a historical period, using two observational precipitation datasets as forcing. Secondly, we generated large ensembles of discharge for calculating risk ratio statistics using the EC-Earth climate model experiments as input. The

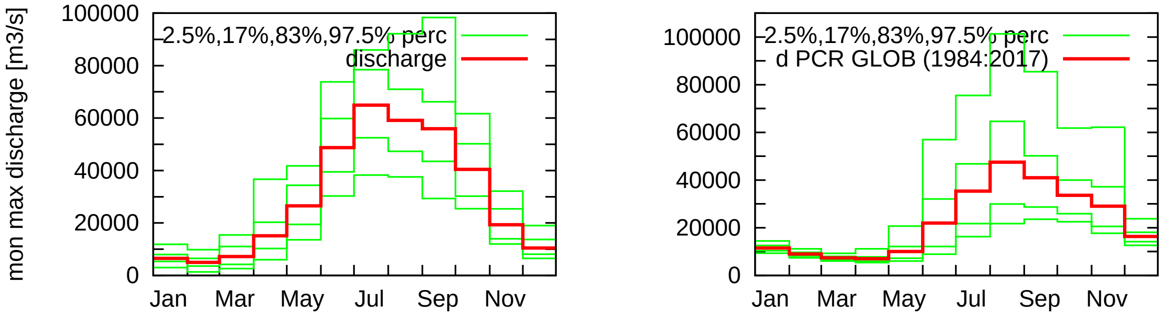

Figure S3. Annual cycle of monthly maximum discharge values for observations (left) and the PCR-GLOBWB model at Bahadurabad, calculated over all years available for observations (1984-2017). The red line shows the mean value, green lines show the 2.5, 17, 83 and 97.5 percentiles.

simulations based on observational data were done at 10 km spatial resolution and provide simulated daily discharge for the Brahmaputra river basin. We used CPC and ERA-interim precipitation estimates for the period 1979-2017 to generate daily fields of soil moisture, groundwater and discharge. The simulations also require temperature and evapotranspiration input, which were taken from ERA-interim for both the CPC and ERA-interim runs. The EC-Earth experiments, i.e. both the 16 transient ensemble members (years 1920-2066 available for 12 members, years 1880-2066 for the other 4 members) and the two time slice experiments (‘present-day’ and ‘2°C-warming’), were used as forcing for PCR-GLOBWB at the coarser resolution of 50 km.

The model version has been extensively validated by Sutanudjaja et al. (2017) and showed a strong agreement between model and observed discharge. The model has been applied in many studies and has shown good performance with regard to simulations of floods (Winsemius et al., 2015), water demand (Wada et al., 2013), drought (Wanders and Wada, 2015a), seasonal teleconnections (Wanders and Wada, 2015b) and reservoir simulations (van Beek et al., 2011). The peak discharge value in the EC-Earth driven model is in August, which is slightly later than in observations but also in the months JAS that are analyzed in this study, see Fig. S3.

4 SWAT

The Soil and Water Assessment Tool (SWAT) is a commonly used hydrological model for investigating climate change impacts on water resources at regional scales (Gassman et al., 2014). This model has already been used to simulate impacts of climate change on the flows of the Brahmaputra River (Mohammed et al., 2017, accepted). The water balance equation used in SWAT consists of daily precipitation, runoff, evapotranspiration, percolation and return flow.

SWAT is a continuous-time hydrological model operating on a daily time step. SWAT is process based, semi-distributed and computationally efficient. In SWAT, the study area is divided into subbasins. These subbasins are then divided into different hydrological response units (HRU) which are the percentage of a subbasin area consisting of unique combined soil, land use and slope properties. After the HRUs are determined, the model calculates the water balance at each HRU using moisture and energy inputs provided by the user.

The water balance equation used in SWAT consists of daily precipitation, runoff, evapotranspiration, percolation and return flow. The simulated flows of all the HRUs in a subbasin are then added together and routed through channels, ponds and reservoirs to the basin outlet. The methods available in SWAT for estimating surface runoff are the Soil Conservation Service (SCS) curve number method and the Green and Ampt infiltration method. Methods for estimating evapotranspiration are the Priestley-Taylor method, the Penman-Monteith method or the Hargreaves method. Methods for estimating flow routing in the river channels are the variable storage coefficient method and the Muskingum routing. Peak runoff is estimated using the modified rational formula. Percolation through each soil layer is estimated using storage routing techniques.

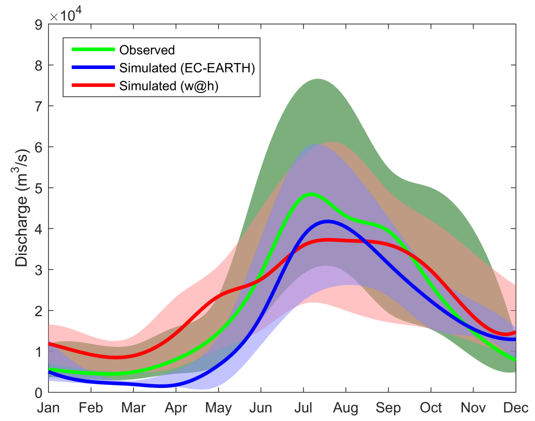

Figure S4. Comparison between monthly observed flows and SWAT simulated flows for both the EC-Earth and the w@h runs at Bahadurabad from 1986-2015.

The SWAT model was used in this study to simulate flows by taking inputs from both the transient and time-slice EC-EARTH experiments and weather@home experiments, using daily maximum and minimum temperatures and precipitation. The parameters of the SWAT model were calibrated twice using climatological data (1986-2015) of each of the two climate models before applying data from the corresponding climate models to simulate flows.

The annual cycle of observed and modelled discharges is shown in Fig. S4. When calibrated with EC-EARTH meteorological data the SWAT model tends to underestimate flows in almost all months of the year. When calibrated with weather@home meteorological data, the SWAT model tends to underestimate flows in the monsoon months while overestimating flows in the remaining months.

5 LISFLOOD

The third hydrological model we use is LISFLOOD. This is a fully distributed and semi-physically based model initially developed by the Joint Research Centre (JRC) of the European Commission in 1997. It was subsequently updated to forecast floods and analyse impacts of climate and land-use change (Burek et al., 2013). It has been used for operational flood forecasts as part of the European Flood Awareness System (EFAS) since 2012 (https://www.efas.eu/about-efas.html). LISFLOOD uses a 1-dimensional channel routing algorithm and solves kinematic wave equations in an implicit manner using four point finite difference solutions to route runoff through the channel network (Knijff et al., 2010). In this study we only used the routing scheme of the model to simulate horizontal water fluxes while the vertical fluxes, surface and subsurface runoff were simulated with the MOSES land surface scheme. The model was run at a spatial resolution of $0.1^\circ \times 0.1^\circ$ and a temporal resolution of a day. It was calibrated with the Parallel version of the Dynamically Dimensioned Search Algorithm (PDDS) (Tolson and Shoemaker, 2007) using an auto-calibration software, Ostrich (Matott, 2017).

The routing scheme of LISFLOOD has been successfully used for flood forecasting at global scale in the Global Flood Awareness System (GloFAS). GloFAS couples LISFLOOD routing scheme with the HTESSEL land surface module (Alfieri et al., 2013). The model can be run at a spatial resolution of 10 km to 100 km and at daily or hourly time steps which makes it suitable for both water balance and flood analysis studies (Knijff et al., 2010). The vertical fluxes, surface and subsurface runoff were simulated with the MOSES land surface scheme. The Met Office Surface Exchange System (MOSES) version 2.2 (Essery et al., 2001) is currently used to produce runoff at the Environmental Change Institute (ECI), University of Oxford for attribution studies.

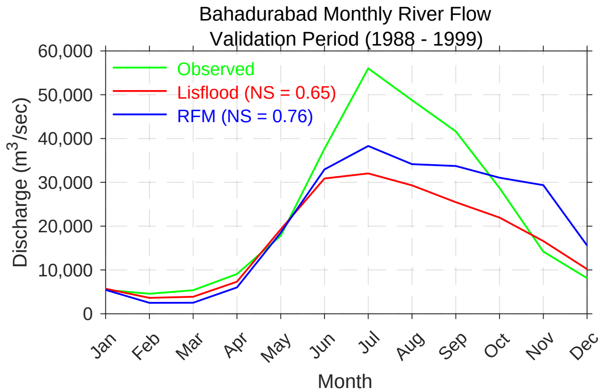

Figure S5. Mean monthly river flow observed at Bahadurabad gauging station and simulated with the LISFLOOD and RFM models. NS stands for Nash and Sutcliffe efficiency.

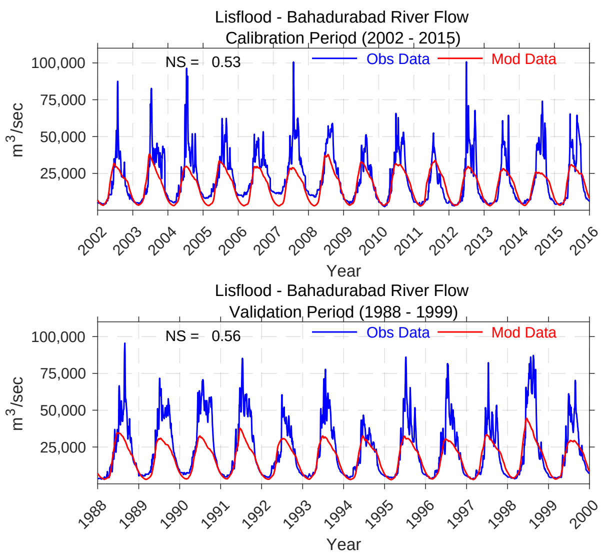

Figure S6. Daily observed and LISFLOOD simulated river flow at Bahadurabad gauging station.

The LISFLOOD model was used in this study to simulate the river flow of the Brahmaputra river at Bahadurabad gauging station with input data from the Weather@home model.

The Nash and Sutcliffe (NS) efficiency of LISFLOOD model for the calibration and validation periods is 0.53 and 0.56 (Fig. S6).

The monthly validation graph shows that the LISFLOOD models is able to simulate the seasonality of rise in spring and summer flows correctly, see Fig. S5. The model underestimates the flows in summer. LISFLOOD simulated the decline in peak flows better than RFM in November and December. Underestimation of flows in summer is mainly because we used ensemble median for calibration of the model parameters which normalized the seasonal peaks.

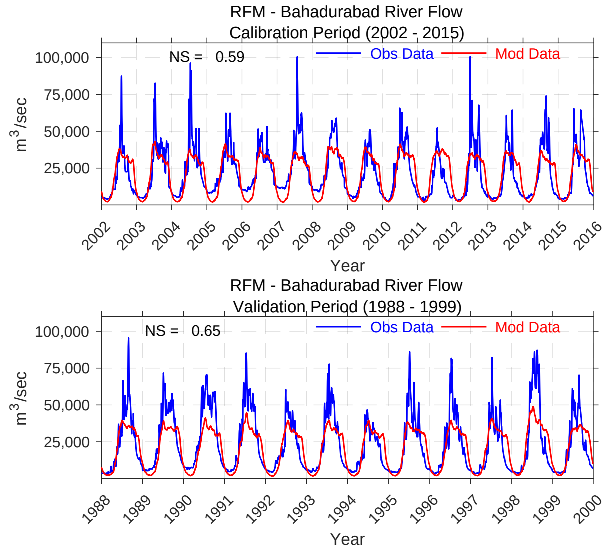

Figure S7. Daily observed and RFM simulated river flow at Bahadurabad gauging station.

6 RFM

The fourth and final hydrological model used in the analysis is a fully distributed River Flow Model (RFM) that estimates the streamflow by discrete approximation of the one-dimensional kinematic wave equation (Dadson et al., 2011). RFM is designed to route the gridded runoff simulated by climate models, land surface schemes (MOSES in our case) or rainfall scenarios to generate river flow at daily or hourly temporal resolution. It has a simple fully distributed spatial structure which makes it possible for it to be coupled with other models. RFM routes the overland flow and stream flow in 2 dimensions and can have different wave speeds for surface and subsurface runoffs. RFM was also calibrated with PDDS and Ostrich.

The RFM routing is achieved by solving the kinematic wave equations separately for the two water sources (Dadson and Bell, 2010). The exchange of runoff between surface and subsurface components, usually at mountain slopes and in the channel network, is estimated as water depth through a return flow variable in the model (Bell et al., 2007). This routing scheme is currently being implemented in the Joint UK Land Environment Simulator (JULES, http://jules-lsm.github.io/vn5.0/namelists/jules_rivers.nml.html).

The RFM model was used in this study to simulate the river flow of the Brahmaputra river at Bahadurabad gauging station with input data from the Weather@home model.

RFM performed better than LISFLOOD with NS values of 0.59 and 0.65 NS for the calibration and validation periods respectively (Figure S7). The monthly validation graph shows that RFM is able to simulate the seasonality of rise in spring and summer flows correctly. The model underestimates the flows in summer but is slightly better than the LISFLOOD simulated river flow. Underestimation of flows in summer is mainly because we used ensemble median for calibration of the model parameters which normalized the seasonal peaks.

References

Alfieri, L., Burek, P., Dutra, E., Krzeminski, B., Muraro, D., Thielen, J., and Pappenberger, F.: GloFAS; global ensemble streamflow forecasting and flood early warning, Hydrology and Earth System Sciences, 17, 1161–1175, https://doi.org/10.5194/hess-17-1161-2013, https://www.hydrol-earth-syst-sci.net/17/1161/2013/, 2013.

Bell, V., Kay, A., Jones, R., and Moore, R.: Development of a high resolution grid-based river flow model for use with regional climate model output, Hydrology and Earth System Sciences, 11, 532–549, http://nora.nerc.ac.uk/id/eprint/1654/, open Access paper. Click official URL for full-text., 2007.

Burek, P., Knijff van der, J., and Roo de, A.: LISFLOOD, distributed water balance and flood simulation model revised user manual 2013, 2013.

Dadson, S. and Bell, V.: Comparison of Grid-2-Grid and TRIP runoff routing schemes, http://nora.nerc.ac.uk/10890/1/dadson_etal_2010_g2gtrip.pdf, 2010.

Dadson, S., Bell, V., and Jones, R.: Evaluation of a grid-based river flow model configured for use in a regional climate model, Journal of Hydrology, 411, 238 – 250, https://doi.org/https://doi.org/10.1016/j.jhydrol.2011.10.002, http://www.sciencedirect.com/science/article/pii/S0022169411006949, 2011.

Donlon, C. J., Martin, M., Stark, J., Roberts-Jones, J., Fiedler, E., and Wimmer, W.: The Operational Sea Surface Temperature and Sea Ice Analysis (OSTIA) system., Remote Sensing of the Environment, 116, 140–158, https://doi.org/10.1016/j.rse.2010.10.017, 2012.

Essery, R., Best, M., and Cox, P.: MOSES 2.2 Technical Documentation, Hadley Centre, Met Office, London Road, Bracknell, Berks R12 2SY, UK, http://jules.jchmr.org/sites/jules.jchmr.org/files/HCTN_30.pdf, 2001.

Gassman, P. W., Sadeghi, A. M., and Srinivasan, R.: Applications of the SWAT Model Special Section: Overview and Insights, Journal of Environmental Quality, 43, 1–8, https://doi.org/10.2134/jeq2013.11.0466, http://dx.doi.org/10.2134/jeq2013.11.0466, 2014.

Guillod, B. P., Jones, R. G., Bowery, A., Haustein, K., Massey, N. R., Mitchell, D. M., Otto, F. E. L., Sparrow, S. N., Uhe, P., Wallom, D. C. H., Wilson, S., and Allen, M. R.: weather@home 2: validation of an improved global–regional climate modelling system, Geoscientific Model Development, 10, 1849–1872, https://doi.org/10.5194/gmd-10-1849-2017, https://www.geosci-model-dev.net/10/1849/2017/, 2017.

Hazeleger, W., Wang, X., Severijns, C., Ştefănescu, S., Bintanja, R., Sterl, A., Wyser, K., Semmler, T., Yang, S., Van den Hurk, B., et al.: EC-Earth V2. 2: description and validation of a new seamless earth system prediction model, Climate dynamics, 39, 2611–2629, 2012.

Knijff, J. M. V. D., Younis, J., and Roo, A. P. J. D.: LISFLOOD: a GIS-based distributed model for river basin scale water balance and flood simulation, International Journal of Geographical Information Science, 24, 189–212, https://doi.org/10.1080/13658810802549154, https://doi.org/10.1080/13658810802549154, 2010.

Massey, N., Jones, R., Otto, F. E. L., Aina, T., Wilson, S., Murphy, J. M., Hassell, D., Yamazaki, Y. H., and Allen, M. R.: weather@home—development and validation of a very large ensemble modelling system for probabilistic event attribution, Quarterly Journal of the Royal Meteorological Society, 141, 1528–1545, https://doi.org/10.1002/qj.2455, https://rmets.onlinelibrary.wiley.com/doi/abs/10.1002/qj.2455, 2014.

Matott, L.: OSTRICH: an Optimization Software Tool, Documentation and User's Guide, www.eng.buffalo.edu/~lsmatott/Ostrich/OstrichMain.html, version 17.12.19, 2017.

Mitchell, D., AchutaRao, K., Allen, M., Bethke, I., Beyerle, U., Ciavarella, A., Forster, P. M., Fuglestvedt, J., Gillett, N., Haustein, K., Ingram, W., Iversen, T., Kharin, V., Klingaman, N., Massey, N., Fischer, E., Schleussner, C.-F., Scinocca, J., Seland, Ø., Shiogama, H., Shuckburgh, E., Sparrow, S., Stone, D., Uhe, P., Wallom, D., Wehner, M., and Zaaboul, R.: Half a degree additional warming, prognosis and projected impacts (HAPPI): background and experimental design, Geoscientific Model Development, 10, 571–583, https://doi.org/10.5194/gmd-10-571-2017, https://www.geosci-model-dev.net/10/571/2017/, 2017.

Mohammed, K., Islam, A. S., Islam, G. T., Alfieri, L., Bala, S. K., and Khan, M. J. U.: Extreme flows and water availability of the Brahmaputra River under 1.5 and 2 °C global warming scenarios, Climatic Change, 145, 159–175, https://doi.org/10.1007/s10584-017-2073-2, https://doi.org/10.1007/s10584-017-2073-2, 2017.

Mohammed, K., A.S., I., Islam, G., Alferi, L., S.K., B., and Khan, M.: Future floods in Bangladesh under 1.5°C, 2°C and 4°C global warming scenarios, Journal of Hydrological Engineering, accepted.

Schaller, N., Kay, A. L., Lamb, R., Massey, N. R., van Oldenborgh, G. J., Otto, F. E. L., Sparrow, S. N., Vautard, R., Yiou, P., Bowery, A., Crooks, S. M., Huntingford, C., Ingram, W. J., Jones, R. G., Legg, T., Miller, J., Skeggs, J., Wallom, D., Weisheimer, A., Wilson, S., and Allen, M. R.: The human influence on climate in the winter 2013/2014 floods in southern England., Nature Climate Change, https://doi.org/10.1038/nclimate2927, 2016.

Sutanudjaja, E. H., van Beek, R., Wanders, N., Wada, Y., Bosmans, J. H. C., Drost, N., van der Ent, R. J., de Graaf, I. E. M., Hoch, J. M., de Jong, K., Karssenberg, D., López López, P., Peßenteiner, S., Schmitz, O., Straatsma, M. W., Vannametee, E., Wisser, D., and Bierkens, M. F. P.: PCR-GLOBWB 2: a 5 arc-minute global hydrological and water resources model, Geoscientific Model Development Discussions, 2017, 1–41, https://doi.org/10.5194/gmd-2017-288, https://www.geosci-model-dev-discuss.net/gmd-2017-288/, 2017.

Taylor, K. E., Stouffer, R. J., and Meehl, G. A.: An Overview of CMIP5 and the Experiment Design, Bull. Amer. Met. Soc., 93, 485–498, https://doi.org/10.1175/BAMS-D-11-00094.1, 2012.

Tolson, B. A. and Shoemaker, C. A.: Dynamically dimensioned search algorithm for computationally efficient watershed model calibration, Water Resources Research, 43, https://doi.org/10.1029/2005WR004723, https://agupubs.onlinelibrary.wiley.com/doi/abs/10.1029/2005WR004723, 2007.

van Beek, L. P. H., Wada, Y., and Bierkens, M. F. P.: Global monthly water stress: 1. Water balance and water availability, Water Resources Research, 47, https://doi.org/10.1029/2010WR009791, http://dx.doi.org/10.1029/2010WR009791, w07517, 2011.

Wada, Y., van Beek, L. P. H., Wanders, N., and Bierkens, M. F. P.: Human water consumption intensifies hydrological drought worldwide, Environmental Research Letters, 8, 034 036, http://stacks.iop.org/1748-9326/8/i=3/a=034036, 2013.

Wanders, N. and Wada, Y.: Human and climate impacts on the 21st century hydrological drought, Journal of Hydrology, 526, 208 – 220, https://doi.org/https://doi.org/10.1016/j.jhydrol.2014.10.047, http://www.sciencedirect.com/science/article/pii/S0022169414008427, drought processes, modeling, and mitigation, 2015a.

Wanders, N. and Wada, Y.: Decadal predictability of river discharge with climate oscillations over the 20th and early 21st century, Geophysical Research Letters, 42, 10,689–10,695, https://doi.org/10.1002/2015GL066929, http://dx.doi.org/10.1002/2015GL066929, 2015GL066929, 2015b.

Winsemius, H. C., Aerts, J. C. J. H., van Beek, L. P. H., Bierkens, M. F. P., Bouwman, A., Jongman, B., Kwadijk, J. C. J., Ligtvoet, W., Lucas, P. L., van Vuuren, D. P., and Ward, P. J.: Global drivers of future river flood risk, Nature Climate Change, 6, 381 EP –, http://dx.doi.org/10.1038/nclimate2893, 2015.